Appl Magn Reson (2012) 43:119–128
DOI 10.1007/s00723-012-0352-7

Applied
Magnetic Resonance

Temperature Dependence of the Proton Overhauser DNP Enhancements on Aqueous Solutions of Fremy's Salt Measured in a Magnetic Field of 9.2 T

Marat Gafurov · Vasyl Denysenkov · Mark J. Prandolini · Thomas F. Prisner

Received: 29 February 2012 / Revised: 25 April 2012 / Published online: 30 May 2012

Abstract The temperature dependence of the water-proton dynamic nuclear polarization (DNP) enhancement from Fremy's salt nitroxide radicals was measured in a magnetic field of 9.2 T (corresponding to 260 GHz microwave (MW) and 392 MHz NMR frequencies) in the temperature range of 15–65 °C. The temperature could be determined directly from the proton NMR line shift of the sample. Very high DNP enhancements of −38 (signal integral) or −81 (peak intensity) could be achieved with a high-power gyrotron MW source. The experimental findings are compared with classical Overhauser theory for liquids, which is based on the translational and rotational motion of the molecules and with molecular dynamics calculations of the coupling factor.

1 Introduction

Dynamic nuclear polarization (DNP) at high magnetic fields has recently gained much interest regarding its potential applications to structural biology, material sciences and analytical chemistry [1–3]. In most applications at high magnetic fields, presently, the polarization transfer from the electron spin to the nuclear spin system has been achieved in the solid state [4, 5]. Direct DNP experiments in the

M. Gafurov · V. Denysenkov · M. J. Prandolini · T. F. Prisner (✉)
Institute of Physical and Theoretical Chemistry and Center for Biomolecular Magnetic Resonance, Goethe University, 60438 Frankfurt am Main, Germany
e-mail: prisner@chemie.uni-frankfurt.de

Present Address:
M. Gafurov
Institute of Physics, Kazan Federal University, 420008 Kazan, Russia

Present Address:
M. J. Prandolini
Helmholtz-Institut Jena, Max-Wien-Platz 1, 07743 Jena, Germany

liquid state were not considered as a valuable option, due to hardware and theoretical problems. Experimentally, the very high dielectric losses of solvents in the liquid phase at high microwave (MW) frequencies cause extensive heating of aqueous samples and strongly limit the MW magnetic field strength inside the sample. This inhibits efficient saturation of the electron spin resonance transition. Theoretically, the Overhauser DNP efficiency [6] is described by [7]:

$$\varepsilon = \xi f_S \frac{\gamma_S}{\gamma_I}. \tag{1}$$

The saturation factor s describes the degree of saturation of the EPR transition, γ_S and γ_I are the gyromagnetic ratios of electron and nuclear spins ($\gamma_S/\gamma_I = -658$ in the case of a proton nuclear spin). The leakage factor f is the fraction of the total nuclear spin relaxation rate due to the non-electron spin interactions and can be easily determined from nuclear magnetic resonance (NMR) relaxation measurements. For radical concentrations in the mM range this factor is approximately 1. The coupling factor ξ is determined by the cross-relaxation rates between the electron and nuclear spin system. These terms rely on a modulation of the hyperfine interaction on the timescale of the inverse electron spin transition frequency. The classical theory, where this spectral density is derived from the translational and rotational motion of the radical and target solvent molecule, predicts a very fast drop of the achievable DNP enhancement at magnetic fields exceeding 0.1 T [7–9]. DNP experiments performed in the 1960s–1980s at magnetic fields between 0.1 and 1.5 T supported this model and allowed the determination of rotational and translational correlation times for many solvents and radicals [10–12].

At high magnetic fields the modulation of the dipolar hyperfine interactions by the translational motion between the solvent molecule and the radical is the dominant source of the DNP mechanism [7]. The translational correlation time τ_t can be calculated for a force-free model of spherical molecules by [13]:

$$\tau_t = \frac{d^2}{D_S + D_R}, \tag{2}$$

where D_S and D_R are the translational diffusion coefficients of solvent molecule and radical, respectively, and d is the distance of closest approach.

Equation (2) describes the major effect of temperature on the DNP enhancement: with increasing temperature, both D_S and D_R will increase, therefore shortening τ_t and increasing the DNP enhancement ε. Additionally, the temperature dependence of the relaxation rates of the electron and nuclear spin might change the saturation factor s and leakage factor f. In this work, we measured the DNP enhancements of water protons with Fremy's Salt as radicals for temperatures between 15 and 65 °C at a magnetic field of 9.2 T. So far, such temperature measurements were done and discussed only up to magnetic fields of $B = 3.4$ T [14, 15]. The high enhancements obtained are compared with predictions based on classical Overhauser theory for liquids, taking translational correlation times extracted from low-field DNP and NMRD experiments [16–20], and calculations of the coupling factor from MD simulations [21, 22].

2 Experimental

All experiments were performed on a 400 MHz Bruker Avance NMR spectrometer, which was extended to a DNP spectrometer by inclusion of a homebuilt 260 GHz MW bridge, based on metallo-dielectric waveguides. It contains a high-power gyrotron MW source (GYCOM) with an output power of 20 W in continuous wave mode at the frequency of 258.9 GHz, and a quasi-optical corrugated waveguide MW transmission line from the MW-bridge to the homebuilt double-resonant DNP probe for aqueous solutions. The total losses from the gyrotron MW source to the resonator are estimated to be of about 6 dB. A more detailed description of the DNP spectrometer is given in the literature [23, 24]. The resonance structure is a cylindrical cavity for the MW, formed by a copper helix, which serves as the NMR coil and is tuned to the 392 MHz proton frequency (Fig. 1). Two plungers coated with a thin silver film confine the MW inside the TE_{011} resonance structure with an active sample length of 1.6 mm. For MW frequency tuning to the electron paramagnetic resonance (EPR) resonance frequency of 260 GHz, one of the plungers can be moved. The MW cavity has two important features: first, it drastically reduces the MW electrical field strength at the sample position, thus avoiding excessive heating of the liquid sample; second, it enhances the MW magnetic field strength B_{MW} at the sample position. ^{15}N-Fremy's salt ($K_2(SO_3)_2NO$, peroxylamine disulfonate), which spontaneously forms a dianion radical upon dissolution into water or alcohol, was synthesized in our group and dissolved in a concentration of 65 mM into water. 50 mM of K_2CO_3 was used as a buffer to reduce the radical decomposition rate. The solvent was bubbled by inert gas (argon) for 15 min to reduce the content of oxygen. The liquid sample was then transferred into 0.03 mm inner diameter quartz capillaries and introduced through the holes in the plungers into the DNP resonator. The total active (MW exposed) sample volume is 1–2 nl. Due to the inhomogeneity caused by metal parts of the MW waveguide and due to the sample geometry, the water proton NMR signals were very broad (in the range of 40–130 Hz). Active sample cooling was achieved by a controlled flow of cold gaseous nitrogen to compensate for the heating caused by MW irradiation and to adjust the temperature of the sample. Temperature monitoring is realized by a

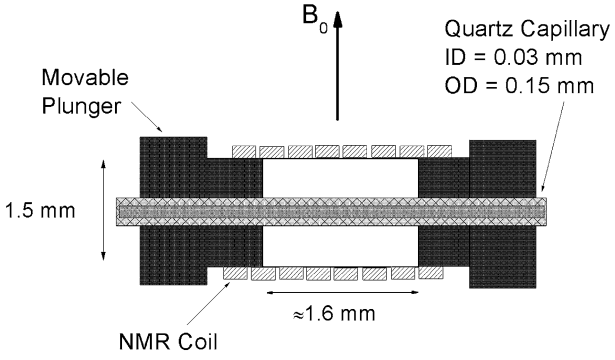

Fig. 1 Schematic representation of the double-resonance structure for DNP at 9.24 T magnetic field

thermocouple placed outside of the resonator and by measuring the known NMR shift of the water protons [25, 26].

3 Results

Figure 2 (top) shows the DNP experiment performed at 260 GHz MW frequency and a sample temperature of 60 °C. The MW power used for this experiment was about 0.6 W; a further increase of the MW power by a factor of 2 did not change the DNP enhancement significantly, but only slightly the NMR line shape due to the MW heating of the sample. This indicates that our applied MW power is large enough to saturate one ^{15}N hyperfine line of the EPR spectra with a linewidth of 3.5 G. Higher MW levels were not applied, in order to avoid boiling of the liquid water sample. The hyperfine splitting of 17.1 G is too large to saturate the other ^{15}N hyperfine line directly, but partial saturation of this second hyperfine line will be achieved by Heisenberg exchange [27, 28]. Under these conditions, a maximum DNP enhancement $\varepsilon_A = -79$ could be achieved comparing signal amplitudes and $\varepsilon_I = -38$ by integrating over the broad NMR line. Room temperature EPR spectra taken at 180 GHz (see Ref. [29] for details of the EPR setup) are shown in Fig. 2

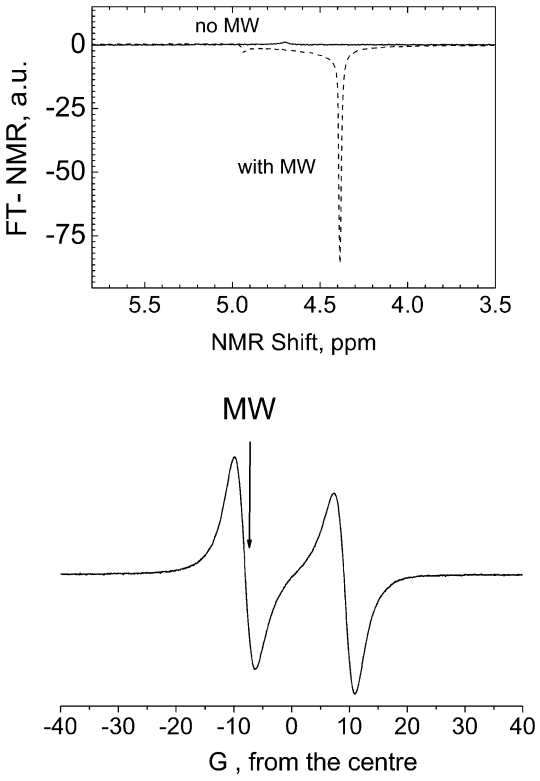

Fig. 2 *Top* ^{1}H NMR/DNP signal from water protons with 65 mM ^{15}N Fremy's Salt, without (positive signal) and with (negative signal) 600 mW of MW power (128 scans, repetition rate 0.5 Hz). The NMR shift of the DNP signal arises from sample heating caused by the MW excitation (60 °C). *Bottom* 180 GHz CW EPR spectrum of aqueous solution of 65 mM ^{15}N Fremy's salt at room temperature. The center field of the scan is 6.4 T. *Arrow* shows a position of MW pumping in DNP experiment

(bottom). The position, where the MW pumping for the DNP experiments at 260 GHz occurred is indicated by an arrow.

Keeping the MW power level constant at 0.6 W, the temperature of the sample was systematically lowered by increasing the flow of the cold N_2, actively cooling the sample. This allowed the determination of the temperature dependence of the DNP enhancement between 15 and 65 °C, keeping the MW power constant (Fig. 3). The NMR temperature shift of −0.012 ppm per °C was measured with a Bruker BBI probe in the temperature range 280–340 K, and is in good agreement with the literature values given for pure H_2O [25, 26] and practically the same for buffer solution or for water with dissolved radicals. The paramagnetic shift, due to the change of the macroscopic magnetization at high MW power [30] was +0.09 ppm, determined by measuring the shift of the position of the NMR line by applying MW irradiation in- and off-resonance with the EPR transition before starting to lower temperature. It is assumed that the temperature dependence of the paramagnetic shift is rather weak in the experimental temperature range. This also defines the accuracy of our temperature measurements on the top of the paramagnetic shift.

4 Discussion

The NMR line shape observed in our experiments (Fig. 2 top) resembles very well the theoretical predictions for long thin cylindrical paramagnetic samples [31]. From this analysis it can be shown that the proton signal from the center of the resonator corresponds to the maximum in the Fourier-transform NMR line. As can be seen in Fig. 3, the peak intensity of the NMR line shows a larger enhancement ε_A compared to the integral over the whole NMR line ε_I. This can be partially explained by the MW field profile within the resonator, which gives higher

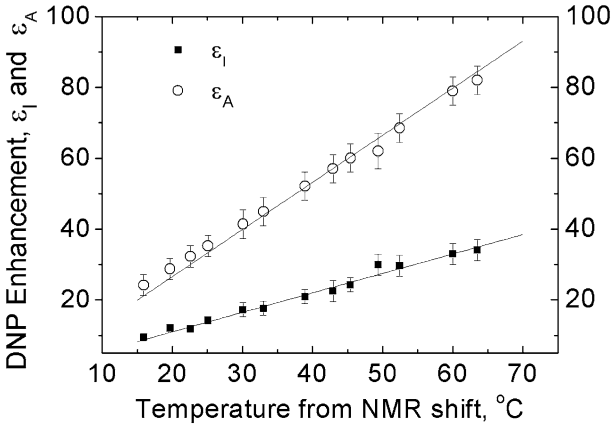

Fig. 3 Temperature dependence of the DNP enhancement factor ε using amplitudes (*circles*) and integrated intensities (*squares*) of the NMR signal ratios with and without MW irradiation. The temperature was extracted from the NMR shift of the water protons. The *lines* with a slope of 1.3/°C (*upper trace*) and 0.55/°C (*lower trace*) describe empirically the experimental findings

saturation factors in the center of the cavity. Additionally, the different MW field strengths along the capillary lead to a temperature gradient over the sample, again intensifying the peak intensity compared to the integral. Finally, the MW excitation close to saturation of the electron spin transition partially suppresses the paramagnetic shift and therefore changes and narrows the NMR line profile. Thus, the DNP enhancement ε_A taken from the maxima of the NMR signal (with/without MW) is an slight overestimate of the maximum achievable DNP enhancement ε, whereas the value taken from the integrated NMR signal ε_I gives a lower bound of this value. In a case of the small droplets placed into the middle of the cavity the values of ε_I tend to be equal ε_A, as it is shown Ref. [15]. Both values obtained in our experiments are the largest DNP enhancements observed so far in liquids at magnetic fields as high as 9.2 T.

To compare our experimentally measured enhancements with predictions of the coupling factor ξ from molecular dynamics (MD) simulations or NMR dispersion (NMRD) experiments, the leakage factor f and the saturation factor s have to be known. This is straightforward for the leakage factor f: the T_1 relaxation time of the water protons with 65 mM Fremy's salt was measured to be 0.13 s at room temperature, resulting in an leakage factor of $f = 0.96$, very close to the optimum value of 1.

The determination of the saturation factor s for Fremy's salt at room temperature and at a magnetic field strength of 9.2 T is by far more difficult: both electron spin relaxation times T_{2e} and T_{1e} have to be known, as well as the Heisenberg exchange rate R_H, the nitrogen nuclear spin relaxation time T_{1N} and the MW magnetic field strength B_{MW}. From the EPR line width of approximately 0.5 G a transverse relaxation time of $T_{2e} \approx 140$ ns can be estimated. The value of the Heisenberg exchange constant was estimated to be $k_{ex} = 1.3 \times 10^9$ M^{-1} s^{-1} at RT from the concentration dependence of the EPR linewidth of ^{14}N Fremy's salt measured between 200 μM and 65 mM at X-band (9 GHz) and at G-band (180 GHz) frequencies (Fig. 4). The literature data varies in the range from $k_{ex} = 0.9 \times 10^9$ M^{-1} s^{-1} at 67 °C [32, 33] up to 2×10^9 M^{-1} s^{-1} at 24 °C [34, 35].

Unfortunately, it is impossible to directly determine the longitudinal relaxation time T_{1e} for our experimental conditions. Relaxation measurements performed on nitroxide radicals at lower magnetic fields (<3.4 T) gave values in the range

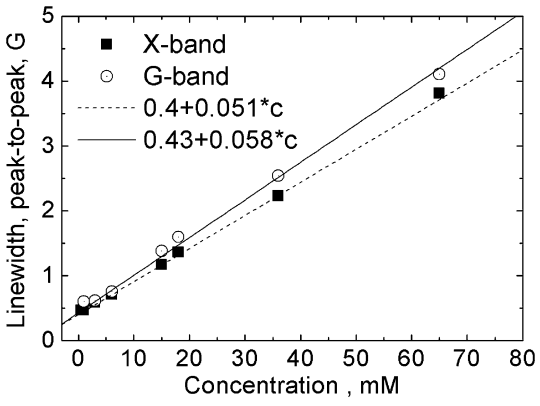

Fig. 4 Concentration dependences of the observed line widths of the central line of aqueous solutions of ^{14}N-Fremy's Salt measured at 300 K at X-band (*solid squares*) and 180 GHz (*open circles*) MW frequencies

between 300 and 800 ns [28, 36]. From a saturation measurement at 9.2 T we estimated a value of $T_{1e} \approx 120$ ns for TEMPOL in water [37]. From measurements at 0.3 T it is known that Fremy's salt has slightly shorter spin–lattice relaxation times compared to TEMPO-type nitroxides: 270–380 versus 300–570 ns, respectively [33, 38]. Therefore, we assumed the longitudinal relaxation time T_{1e} to be in the range between 120 and 350 ns. Our MW excitation field strength B_{MW} was in the range of 2.5–3 G for our experimental conditions, calculated from the conversion factor of our MW resonator [22, 23]. The distribution of the MW field along the cavity axis has been determined from the corresponding waveguide solution for TE_{011} mode [39]. Taking all these values along with the known components of *g*- and *A*-tensors [35], we can calculate by a density matrix approach [27] that the saturation factor *s* for our maximal B_{MW} field strengths is in the range between 0.65 and 0.85. Taking the excitation profile of our MW resonator into account, we obtain an integral saturation factors between 0.4 and 0.7 (Fig. 5).

With the so determined leakage factors *f* and average saturation factors s_{av}, quantitative comparison with coupling factors determined from MD simulations [22] and NMRD experiments [33] is possible. The temperature-dependent coupling factors for upper and lower estimates of the saturation factors are shown together with the MD calculated values in Fig. 6. As can be seen the values for the coupling factor extracted from experimental DNP enhancements taking the upper limit for the expected saturation factor agree rather well with the coupling factors predicted by MD calculations. From the diffusion correlation time τ_D between 29 and 31 ps, calculated from NMRD measurements at 25 °C [33] a coupling factor of $1.5–1.7 \times 10^{-2}$ can be calculated for 9.2 T magnetic field; somewhat lower than the values obtained from MD simulations and estimated from our experiments. The temperature dependence of the MD simulations and experimental values agree

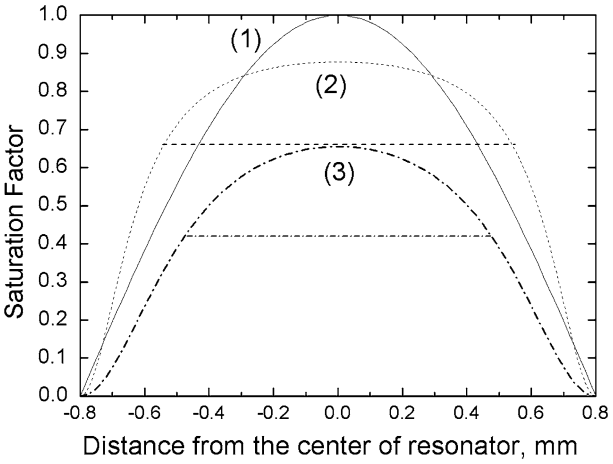

Fig. 5 (*1*) Normalized MW B_{MW} field along the axis of the resonator; (*2*) calculated saturation factor along the axis of the resonator with $T_{1e} = 350$ ns and $B_{MW}^{max} = 3$ G resulting in averaged $s_{max\ av} = 0.66$ (*horizontal dashed line*); (*3*) the same with $T_{1e} = 120$ ns and $B_{MW}^{max} = 2.5$ G resulting in $s_{min\ av} = 0.42$ (*horizontal dot-dashed line*)

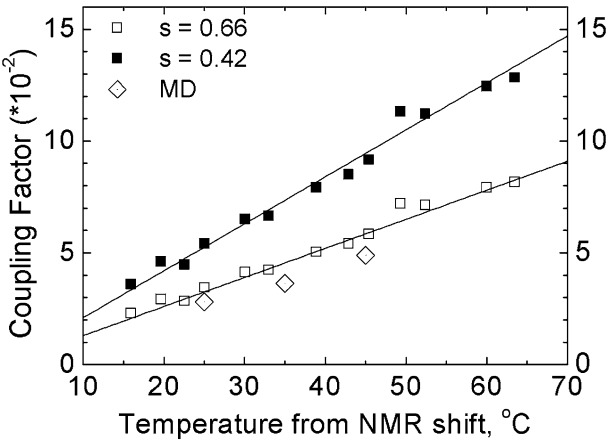

Fig. 6 Temperature dependence of coupling factor: experimental enhancements ε_I using $s = 0.66$ (*open squares*), experimental ε_A with $s = 0.42$ (*full squares*), MD data from Ref. [21] (*open diamonds*). The *straight lines* with the slopes of 0.13/°C (*lower trace*) and 0.21/°C (*upper trace*) are just guides for the eye

extremely well. Thus, for this concentration and MW power, the temperature dependence of the DNP enhancements seems to be dominated by the temperature dependence of the coupling factor alone. Indeed, the measured leakage factor f does not depend on temperature in the range from 283 to 333 K. The temperature independence of the saturation factor for Fremy's salt with the given concentration might be caused by partial cancelation of effects: whereas the Heisenberg exchange rate will increase with higher temperature, the longitudinal relaxation time T_{1e} will shorten.

5 Conclusion

Very high DNP enhancements have been observed with Fremy's salt dissolved in water at a magnetic field of 9.2 T. Differences between enhancement factors calculated from the signal amplitude and signal integral can be rationalized by the excitation profile, temperature gradient and the influence of the paramagnetic molecules on the proton NMR lineshape. The achieved enhancements can only qualitatively be compared with predicted coupling factors from MD simulations, because the saturation factor could not be determined independently. Improvements of the experimental setup are under way, allowing more accurate independent determination of this factor. The enhancements obtained seem to exceed the expectations based on known translational diffusion constants and MD predictions. More systematic investigations with different radicals and solvents in this direction are under way. The high enhancements achieved in the liquid state at high magnetic fields offer interesting applications for applications on samples with restricted size, which might find applications, for example, in analytical chemistry and metabolite investigations, micro-chips and screening arrays.

Acknowledgments We thank Bernhard Thiem and Burkhard Endeward, for experimental support and Dominik Margraf for the synthesis of ^{15}N Fremy's Salt. We are indebted to Deniz Sezer for discussion and theoretical support. Frank Engelke, Alexander Krahn and Thorsten Marquartsen (Bruker BioSpin) are thanked for technical support. Financial support by the design study project BIO-DNP (European Commission) and the German–Israel Project DIP OS 106/12-1 (German Research Society) are gratefully acknowledged.

References

1. W. Köckenberger, T.F. Prisner, Appl. Magn. Reson. **34**, 213 (2008)
2. R.G. Griffin, T.F. Prisner, Phys. Chem. Chem. Phys. **22**, 5725 (2010)
3. V.A. Atsarkin, J. Phys. **324**, 012003 (2011)
4. L.R. Becerra, G.J. Gerfen, R.J. Temkin, D.J. Singel, R.G. Griffin, Phys. Rev. Lett. **71**, 3561 (1993)
5. J.H. Ardenkjaer-Larsen, B. Fridlund, A. Gram, G. Hansson, L. Hansson, M.H. Lerche, R. Servin, M. Thaning, K. Golman, Proc. Natl. Acad. Sci. USA **100**, 10158 (2003)
6. A.W. Overhauser, Phys. Rev. **92**, 411 (1953)
7. K.H. Hausser, D. Stehlik, Adv. Magn. Reson. **3**, 79 (1968)
8. A. Abragam, *The Principles of Nuclear Magnetism*, (Clarendon Press, Oxford, 1961)
9. W. Müller-Warmuth, K. Meise-Gresch, Adv. Magn. Reson. **11**, 1 (1983)
10. R.A. Dweck, R.E. Richards, D. Taylor, Ann. Rev. NMR. Spectrosc. **2**, 293 (1969)
11. J. Potenza, Adv. Mol. Relax. Proc. **4**, 229 (1972)
12. R.A. Wind, M.J. Duuvestun, C. Van Der Lugt, A. Manenschun, J. Vriend, Prog. NMR Spectrosc. **17**, 33 (1985)
13. J.H. Freed, J. Chem. Phys. **68**, 4034 (1978)
14. E.V. Kryukov, K.J. Pike, T.K.Y. Tam, M.E. Newton, M.E. Smith, R. Dupree, Phys. Chem. Chem. Phys. **13**, 4372 (2011)
15. P.J.M. van Bentum, G.H.A. van der Heijden, J.A. Villanueva-Garibay, A.P.M. Kentgens, Phys. Chem. Chem. Phys. **13**, 17831 (2011)
16. B.D. Armstrong, S. Han, J. Chem. Phys. **127**, 104508 (2007)
17. B. Borah, R.G. Bryant, J. Chem. Phys. **75**, 3297 (1981)
18. E. Goldammer, W. Kreysch, H. Wenzel, J. Sol. Chem. **7**, 197 (1978)
19. P. Höfer, G. Parigi, C. Luchinat, P. Carl, G. Guthausen, M. Reese, T. Carlomagno, C. Griesinger, M. Bennati, J. Am. Chem. Soc. **130**, 3254 (2008)
20. M. Bennati, C. Luchinat, G. Parigi, M.-T. Türke, Phys. Chem. Chem. Phys. **12**, 5902 (2010)
21. D. Sezer, M.J. Prandolini, T.F. Prisner, Phys. Chem. Chem. Phys. **11**, 6626 (2009)
22. V.P. Denysenkov, M.J. Prandolini, M. Gafurov, D. Sezer, B. Endeward, T.F. Prisner, Phys. Chem. Chem. Phys. **12**, 5786 (2010)
23. V.P. Denysenkov, M.J. Prandolini, A. Krahn, M. Gafurov, B. Endeward, T.F. Prisner, Appl. Magn. Reson. **34**, 289 (2008)
24. M.J. Prandolini, V.P. Denysenkov, M. Gafurov, B. Endeward, T.F. Prisner, J. Am. Chem. Soc. **131**, 6090 (2009)
25. Q. Teng, *Structural Biology: Practical NMR Applications* (Springer, New York, 2005), p. 19
26. T. Wu, K.R. Kendell, J.P. Felmlee, B.D. Lewis, R.L. Ehman, Med. Phys. **27**, 221 (2000)
27. D. Sezer, M. Gafurov, M.J. Prandolini, V.P. Denysenkov, T.F. Prisner, Phys. Chem. Chem. Phys. **11**, 6638 (2009)
28. M.-T. Türke, I. Tkach, M. Reese, P. Höfer, M. Bennati, Phys. Chem. Chem. Phys. **12**, 5893 (2010)
29. M.M. Hertel, V.P. Denysenkov, M. Bennati, T.F. Prisner, Magn. Res. Chem. **43**, 248 (2005)
30. R. Wind, H. Lock, M. Mehring, Chem.Phys.Lett. **141**, 283 (1987)
31. E. Belorizky, W. Gorecki, M. Jeannin, P.H. Fries, P. Maldivi, E. Gout, Chem. Phys. Lett. **175**, 579 (1990)
32. B. Bales, M. Peric, J. Phys. Chem. B **101**, 8707 (1997)
33. M.-T. Türke, G. Parigi, C. Luchinat, M. Bennati, Phys. Chem. Chem. Phys. **14**, 502 (2012)
34. M.P. Eastman, G.V. Bruno, J.H. Freed, J. Chem. Phys. **52**, 2511 (1970)
35. S.A. Goldman, G.V. Bruno, C.F. Polnaszek, J.H. Freed, J. Chem. Phys. **56**, 716 (1972)
36. W. Froncisz, T.G. Camenisch, J.J. Ratke, J.R. Anderson, W.K. Subczyski, R.A. Strangeway, J.H. Sibradas, J.S. Hyde, J. Magn. Reson. **193**, 297 (2008)

37. M.J. Prandolini, V. Denysenkov, M. Gafurov, S. Lyubenova, B. Endeward, M. Bennati, T. Prisner, Appl. Magn. Reson. **34**, 399 (2008)
38. M. Dutka, R.J. Gurbiel, J. Kozioł, W. Froncisz, J. Magn. Res. **170**, 220 (2004)
39. R.E. Collin, *Foundautions for Microwave Engineering*, (McGraw-Hill, 1992), pp. 505–506